THE JOURNAL OF PHYSICAL CHEMISTRY C

Article

pubs.acs.org/JPCC

Reversible Photoinduced Formation and Manipulation of a Two-Dimensional Closely Packed Assembly of Polystyrene Nanospheres on a Metallic Nanostructure

Tatsuya Shoji,[†] Michiko Shibata,[‡] Noboru Kitamura,[†,‡] Fumika Nagasawa,[‡] Mai Takase,[‡] Kei Murakoshi,[†,‡] Atsushi Nobuhiro,[§] Yoshihiko Mizumoto,[§] Hajime Ishihara,[§] and Yasuyuki Tsuboi*[,†,‡,∥]

[†]Department of Chemistry, Graduate School of Science, Hokkaido University, Sapporo 060-0810, Japan,

[‡]Graduate School of Chemical Sciences and Engineering, Hokkaido University, Sapporo 060-0810, Japan

[§]Department of Physics and Electronics, Osaka Prefecture University, 1-1, Gakuen-cho, Nakaku, Sakai, Osaka 599-8531, Japan

[∥]JST (Japan Science and Technology Cooperation), PRESTO, Japan

Supporting Information

ABSTRACT: Nanostructure-enhanced optical trapping of polymer beads was investigated by means of fluorescence microspectroscopy. It was found that trapping behavior was quite sensitive to the particle size as well as excitation light intensity. We present a 2D closely packed assembly of polystyrene nanospheres on a gold nanostructure that is triggered by gap-mode localized surface plasmon (LSP) excitation. We discuss the trapping mechanism from the viewpoints of not only the radiation force but also of the thermal force (thermophoresis and thermal convection) induced by near-infrared laser irradiation. Thermophoresis worked as a repulsive force whose direction was opposed to that of the radiation force. On the other hand, thermal convection acted in favor of trapping: It supplied nanospheres toward the LSP excitation area. By suppressing the repulsive force, the assembled trapped nanospheres took the form of hexagonal shapes on a gold nanostructure. By optimizing irradiation parameters, we achieved 2D manipulation of nanospheres on a substrate. Our method has advantages over the conventional optical tweezers technique because of its weak light intensity, and could be a promising method of creating and manipulating a 2D colloidal crystal on a plasmonic substrate.

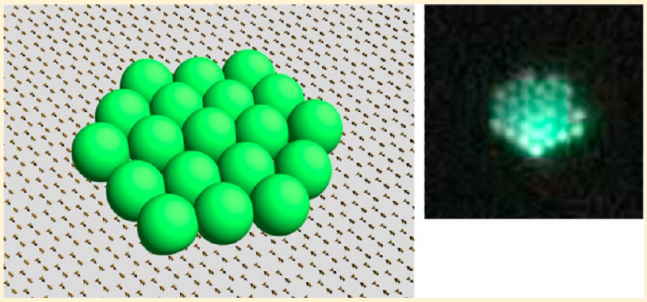

INTRODUCTION

Localized surface plasmons (LSP) have been investigated because they demonstrate highly sensitive spectroscopies[1−5] and the enhancement of photochemical reactions.[6−10] These applications are enabled by the enhancement effect of an incident resonant electromagnetic field (EMF) at the surfaces of noble metallic nanostructures.[11−13] In particular, the application of LSPs at the nanogaps between adjacent noble metallic nanostructures (gap-mode LSP) has recently attracted much attention for achieving the effective optical trapping (OT) of nanoparticles at the nanogaps; this is known as LSP-based OT (LSP-OT). Since Grigorenko et al. first experimentally demonstrated the LSP-OT of polystyrene microspheres in 2008,[14] various researchers have been exploring the phenomenon to reveal the features and mechanisms of the LSP-OT of polymer beads, metallic nanoparticles, and bacteria.[15−24] We also demonstrated the LSP-OT of semiconductor nanocrystals (quantum dots) and polystyrene nanospheres and by means of confocal fluorescence microspectroscopy.[22−24] Such LSP-OT has a great advantage with respect to incident light intensity: the laser intensity can be much decreased (to the order of kW/cm^2) and still achieve stable trapping, as compared to conventional optical tweezers (∼MW/cm^2).[25−29] Thus, LSP-OT could enable a new technique for manipulating not only nanoparticles but also smaller molecules such as polymer chains,[24] proteins, and DNA.

According to recent research, however, the process of LSP-OT should not be so simple. Simultaneously with LSP excitation, other favorable or unfavorable physical processes take place competing with the enhanced radiation force (RF), which is the driving force for OT. We currently consider that photothermal effects (local temperature elevation around plasmonic nanostructures) upon LSP excitation make a significant contribution in LSP-OT. In general, LSP excitation should lead to heat generation in competition with EMF enhancement. Wu and Gan pointed out that, theoretically,

Special Issue: Nanostructured-Enhanced Photoenergy Conversion

Received: June 29, 2012
Revised: August 23, 2012
Published: September 5, 2012

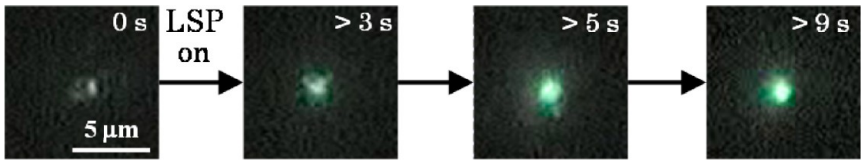

Figure 1. Fluorescence micrographs of trapping behavior of PsNs (d = 0.1 μm) based on gap-mode LSP (NIR light intensity, 2.0 kW/cm^2). 0 s means the time just before starting NIR laser irradiation, and the time in the images expresses NIR laser irradiation time.

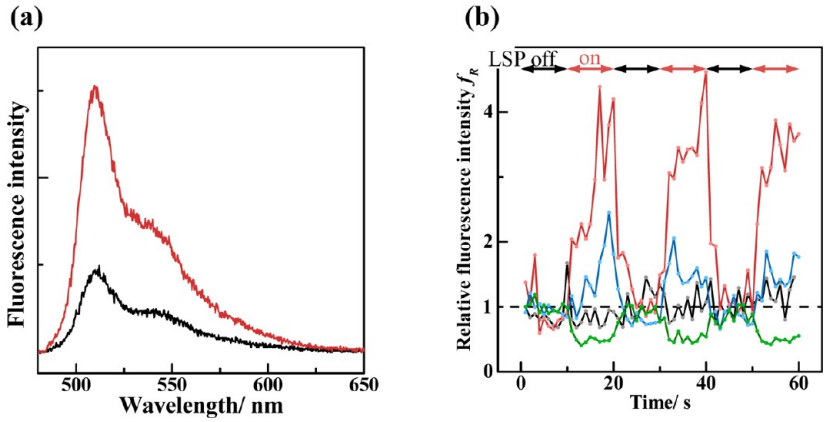

Figure 2. Fluorescence modulation of PsNs (d = 0.1 μm) by NIR laser irradiation. (a) Fluorescence spectra obtained without (black) and with NIR laser irradiation (red line, I_{NIR} = 2.0 kW/cm^2). (b) Temporal profile of the relative fluorescence intensity f_R upon on-and-off repetitive NIR laser irradiation (repetition time ≈ 10 s) at 2.0 (red), 8.0 (blue), and 11 kW/cm^2 (green line) together with f_R without NIR irradiation as a reference (black). Fluorescence spectra were acquired at 3.8 ms time intervals with an exposure time of 1.0 s.

photothermal effects can be regarded as unfavorable for LSP-OT.[30] Various approaches have been reported to avoid these effects: reducing the density of plasmonic nanostructures in the irradiation area,[15] creating plasmonic nanostructures on a heat sink,[17] and selecting a light wavelength that is off-resonant for LSP.[21] On the other hand, in one study on LSP-OT, Roxworthy et al. found experimentally that lateral thermal convection supports the LSP-OT of polystyrene nanospheres, resulting in multiple trapping even around the outside of the irradiation area.[21] It should be noted that LSP-OT mechanisms that involve photothermal effects have only recently begun to be discussed, and hence the details still remain unclear.

In the present study, we demonstrated the LSP-OT of fluorescent-labeled polystyrene nanospheres (PsNs) with a variety of sizes. PsNs are fundamental model targets for optical trapping studies. We discussed LSP-OT of PsNs, taking the thermal forces into account. Furthermore, we demonstrated multiple optical trapping in which a closely packed 2D hexagonal assembly appeared on a metallic nanostructure. On the basis of the optimum trapping condition that we revealed, we succeeded in 2D-optical manipulation of PsNs on a metallic nanostructure. The availability of LSP-OT would open a new channel for easily creating tools for 2D colloidal crystals and for patterning structures more precisely.

EXPERIMENTAL SECTION

To create a plasmonic substrate, gold nanopyramidal-dimer arrays were fabricated on glass substrates (coverslips) by means of angular-resolved nanosphere lithography (AR-NSL). We have already described the features of this AR-NSL substrate, such as morphology, spectroscopy, and spatial distributions of enhanced EMF in detail (the morphology of the substrate is shown and explained in Supporting Information).[22−24] The AR-NSL substrate has a broad extinction band around 800 nm that corresponds to a resonant transition of a gap-mode LSP.

As target objects to be optically trapped, we used PsNs (diameter d = 1.0 μm, Funakoshi Co., Ltd.) and dye-doped PsNs (Molecular Probes, Fluospheres F8803, F8811, F8813) whose diameters were 0.1, 0.2, and 0.5 μm, respectively. The dye molecules in the PsNs have an absorption band around 505 nm and an emission band around 515 nm. The PsNs were homogeneously dispersed in water at certain concentrations: ca. 3.6 × 10^{10} (d = 0.1 μm), 9.1 × 10^9 (d = 0.2 μm), 5.8 × 10^8 (d = 0.5 μm), and 4.5 × 10^9/ml (d = 1.0 μm), respectively. It should be noted that the concentrations were suppressed to prevent aggregation of the PsNs with each other; namely, colloidal crystals were not formed spontaneously. The PsNs-dispersed solutions (d = 0.1 μm) were filtered through a 0.2 μm syringe filter to eliminate microdusts (dusts, impurities, and aggregates of spheres) in the solutions. 50 μl samples of the PsNs-dispersed solutions were placed between a holed glass slide (maximum depth ∼300 μm) and the AR-NSL substrate.

For observation of LSP-OT, we used a confocal fluorescence microscope as described in our previous literature.[22,24] We chose two laser beams: a continuous wave (cw) near-infrared (NIR) diode laser (λ = 808 nm, Spectra Physics, CWA0400-SXD-808−30-E) was used for gap-mode LSP excitation of the AR-NSL substrates, and a cw visible Ar$^+$ laser (λ = 488 nm, Ion Laser Technology, 5490ASL) was used for fluorescence excitation of the dye molecules in the PsNs, respectively. The NIR laser was loosely focused on the AR-NSL substrate with an irradiation area of 2 × 10^{-7} cm^2 (circular shape with d = 5.0 μm), while the Ar$^+$ laser was tightly focused to the diffraction limit (d = 0.5 μm) and its irradiation position was the center of the NIR focal spot. We determined the cw NIR laser intensity (I_{NIR} in kW/cm^2) at the focal point where the light was passed through an objective lens (oil-immersion, ×100, N.A. = 1.30,

dx.doi.org/10.1021/jp306405j | J. Phys. Chem. C 2013, 117, 2500−2506

Nikon). In such an optical setup, the number of excited nanogaps is ~1000 in the NIR irradiation area and ~10 in the Ar^+ irradiation area, respectively. All of the experiments were performed under ambient conditions at room temperature.

RESULTS AND DISCUSSION

NIR Laser Intensity Dependence of Optical Trapping Behavior. Figure 1 includes a series of optical micrographs showing the representative optical trapping behavior of PsNs (d = 0.1 μm). Before LSP excitation (with Ar^+ laser irradiation but without NIR laser irradiation), we observed Brownian motion of the PsNs as a "fuzzy green" fluorescence image at the focal spot of the Ar^+ laser. Upon LSP excitation with NIR irradiation (I_{NIR} = 2.0 kW/cm^2), the brightness of the fluorescence seemed to be constant, after which it gradually increased with irradiation time. Such behavior was similar to that observed in our previous report,[22] indicating that PsNs were optically trapped on the AR-NSL substrate due to RF enhanced by LSP. It should be noted that LSP-OT of PsNs was achieved with weak NIR laser irradiation (2.0 kW/cm^2). Upon switching off the NIR irradiation, we observed a decrease in fluorescence intensity that corresponded to the migration of PsNs from the focal point.

In order to follow such behavior qualitatively, microscopic fluorescence spectroscopy was carried out (Figure 2a). The fluorescence intensity upon LSP excitation (red line) was obviously higher than that before the excitation (black line). We can safely attribute the increase in fluorescence intensity to an increase in the number of PsNs at the focal spot induced by trapping. From fluorescence spectra, we obtained a time trace of relative fluorescence intensity (f_R) (Figure 2b). The unity of f_R (f_R = 1) is defined as fluorescence intensity with Ar^+ laser irradiation but without NIR laser irradiation. The gray line in the figure shows f_R without NIR laser irradiation during the measurement time. f_R qualitatively corresponds to the number of PsNs at the focal point. Here, f_{on} is defined as f_R upon LSP excitation. In the measurements, LSP was excited for durations of 10−20, 30−40, and 50−60 s, respectively. At I_{NIR} ~ 2.0 kW/cm^2 (red line), f_{on} became clearly higher than f_{off} (f_R without LSP excitation). From a simplistic consideration, f_{on} would be expected to increase with increasing I_{NIR} because RF is proportional to the incident light intensity. Contrary to our expectation, f_{on} at I_{NIR} ~ 8.0 kW/cm^2 (blue line) was lower than that at 2.0 kW/cm^2. At I_{NIR} ~ 11 kW/cm^2 (green line), f_{on} was lower than 1 unity; namely, PsNs were not trapped but were excluded from the focal point. These experimental results deviating from the single prediction imply a possibility that LSP-OT is disturbed by a repulsive effect that becomes applicable with increasing I_{NIR}.

We measured the I_{NIR} dependence of f_{on} for d = 0.1 (red circles) and 0.2 μm (blue circles) PsNs to clarify such an effect in detail (Figure 3a). The error bars in the figure include the fluctuations of f_{on} seen in Figure 2, and each data point was determined by averaging. Interestingly, we found an optimum NIR laser intensity for achieving an efficient LSP-OT. For 0.1 μm PsNs, f_{on} became higher with increasing I_{NIR} below 2.0 kW/cm^2. However, f_{on} then decreased when I_{NIR} was above 2.0 kW/cm^2. Over 10 kW/cm^2, f_{on} was smaller than 1 throughout the observation, which indicates the exclusion of PsNs from the focal spot by LSP excitation. The I_{NIR} dependence of f_{on} for 0.2 μm PsNs exhibited a tendency similar to that of 0.1 μm PsNs. In the case of d = 0.5 μm PsNs, the number of PsNs at the focal point can be directly counted using microscopic observation (see later, Figure 6).

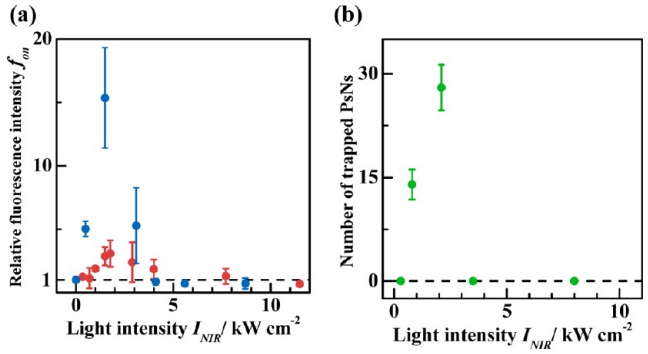

Figure 3. (a) NIR laser intensity dependences of f_{on} of d = 0.1 (red circles) and 0.2 μm (blue circles) PsNs. (b) NIR laser intensity dependences of the number of trapped d = 0.5 μm PsNs. We directly counted the number of 0.5 μm PsNs trapped in the NIR irradiation area.

In Figure 3b, the vertical axis expresses the number of 0.5 μm PsNs in the NIR irradiation area, because the PsNs were stably trapped and assembled as described in a later section. This expression instead of f_{on} provides us with more precise information, because f_{on} is obtained from only the Ar^+ laser irradiation area which is much smaller than the NIR irradiation area (see the Experimental Section). Again here, the number of trapped PsNs reached a maximum at I_{NIR} = 2.0 kW/cm^2. This is the common behavior, irrespective of the size of the PsNs, that the optimum NIR laser intensity is approximately 2.0 kW/cm^2. On the other hand, the trapping efficiency clearly depends on the size of the PsNs. The maximum f_{on} for 0.2 μm PsNs (f_{on} ~ 15) was obviously higher than that for 0.1 μm PsNs (f_{on} < 5). This result suggests that RF is more efficiently exerted on 0.2 μm PsNs than on 0.1 μm PsNs.

Here, we briefly summarize the characteristics of the experimental results for the I_{NIR} dependence of f_{on}: (i) f_{on} increased with increasing I_{NIR}, (ii) f_{on} decreased when I_{NIR} was over a certain I_{NIR} value (2.0 kW/cm^2), (iii) the maximum of f_{on} increased with increasing diameter of the PsNs, and (iv) strong NIR laser irradiation led to the exclusion of PsNs from the NIR irradiation area. These results suggest that NIR irradiation would induce not only an attractive force (RF) but also a repulsive force that was exerted on the PsNs at the focal point. These forces would be explained on the basis of RF and thermal forces. In the next section, we discuss the LSP-OT mechanism on the basis of these forces.

Discussion on the Mechanism of Optical Trapping of Nanospheres. *Radiation Force.* First, we considered the RF exerted on PsNs, which can be expressed by the following equations:

$$\mathbf{F}_{RF} = \frac{1}{2}\alpha \mathbf{E}^2 \quad (1)$$

$$\alpha = 4\pi\varepsilon_2 r^3 \frac{(n_1/n_2)^2 - 1}{(n_1/n_2)^2 + 2} \quad (2)$$

where $\mathbf{F}_{RF}$ is the RF (dipole gradient force), $\mathbf{E}$ is the electric field, and α is the polarizability of a particle to be trapped. In eq 2, r is the radius of the particle, ε_2 is the dielectric constant of the surrounding medium, and n_1 and n_2 are the refractive index of the particle and the surrounding medium, respectively.

dx.doi.org/10.1021/jp306405j | J. Phys. Chem. C 2013, 117, 2500−2506

According to eqs 1 and 2, RF becomes higher with increasing size of the trapped particle. Therefore, it is natural that the maximum of f_{on} increases as we expected the diameter of the PsNs. On the basis of eqs 1 and 2, it is also reasonable that f_{on} increases with increasing NIR laser intensity. Above 2.0 kW/cm^2, however, f_{on} was inversely proportional to the NIR laser intensity. This behavior could be ascribed to an unknown repulsive force, which works to destabilize the LSP-OT. We consider that the repulsive force is due to photothermal effects induced by NIR irradiation. In the following section, we discuss the repulsive force together with RF on the basis of the results of theoretical calculations.

Thermophoresis. In general, metallic nanostructures under LSP excitation generate heat through lattice relaxation. Such photothermal effects on plasmonic phenomena have recently been discussed in several studies.[4,13,31−34] However, a precise temperature elevation ΔT was rarely evaluated, since the gradients of the local temperatures around plasmonic nanostructures could be huge. For discussion of the thermal effect, El-Sayed et al. measured the bulk temperature of sample solutions containing gold nanoparticles.[33] Misawa et al. recently evaluated the local temperature just on the surface of a gold nanoblock by measuring the intensity ratio of the Stokes/anti-Stokes SERS signals of a dye.[34] Wu and Gan also numerically calculated the spatial distribution of temperature around gold nanopillars with a nanogap upon plasmon excitation.[30] Recently, we carried out fluorescence correlation spectroscopy (FCS) to evaluate the local temperature elevation ΔT in the vicinity of an AR-NSL substrate. At I_{NIR} = 1.0 kW/cm^2, we determined ΔT to be 8−9 K.[24] Such temperature elevation corresponds to a huge temperature gradient (∼10^5 K/m), resulting in thermophoresis (thermodiffusion or Ludwig−Soret effect) and thermal convection (Rayleigh−Bénard convection).

Thermophoresis moves particles along a temperature gradient.[35−37] Recently, an experimental method using an accurate optical probing technique was developed for investigating thermophoretic phenomena in colloidal fluid systems such as surfactant micelles and polymer latex micro- and nanospheres in solution. In particular, PsNs are fundamental model targets for revealing the thermophoresis mechanism.[38] Namely, we can precisely estimate the net force exerted on PsNs in a temperature gradient; this is known as the thermal force, $\mathbf{F}_{Th}$. The calculation method of thermal force $\mathbf{F}_{Th}$ exerted on 0.1 μm PsNs was described in the Supporting Information. It should be noted that the thermal force $\mathbf{F}_{Th}$ is a repulsive force whose direction is opposed to that of RF $\mathbf{F}_{RF}$. For the theoretical calculation of RF $\mathbf{F}_{RF}$ exerted on 0.1 μm PsNs, we solved the enhanced EMF strength of the incident light around the gold nanopyramidal dimers on the basis of a discrete dipole approximation (details were described in the previous literature[22−24]). Figure 4 shows the I_{NIR} dependence of $|\mathbf{F}_{Th}|$ (red circles) and $|\mathbf{F}_{RF}|$ (blue squares) for 0.1 μm PsNs at 10 nm far from the AR-NSL surface (the model for the calculation was illustrated in the Supporting Information). It is clear that RF was comparable to the thermal force at light intensities up to 2.0 kW/cm^2; $|\mathbf{F}_{RF}| \approx |\mathbf{F}_{Th}|$. Above 2.0 kW/cm^2, the thermal force overcomes RF; $|\mathbf{F}_{RF}| < |\mathbf{F}_{Th}|$. Such results could provide a reasonable explanation for the experimental observation seen in Figure 3. Thus, in order to reveal the overall LSP-OT behavior totally, we should take into account not only RF but also the thermal force.

Thermal Convection. As a result of local temperature elevation, it is natural to consider a contribution from thermal convection (Rayleigh−Bénard convection). Indeed, such thermal convection has been pointed out in plasmonic excitation.[39] Using 1.0 μm PsNs and AR-NSL substrates, we successfully visualized particle transportation induced by thermal convection, as shown in Figure 5 (see also a movie in the Supporting Information). Before turning on LSP excitation, the PsNs fluctuated due to Brownian motion. Upon LSP excitation (I_{NIR} ∼ 20 kW/cm^2), the PsNs tried to approach the irradiation area from outside of the area. In the figure, we show representative trajectories of the PsNs. In such movement, the velocity of the PsNs was estimated to be ∼5 μm/s. The PsNs were attracted into the irradiation area along the lateral axis (parallel to the substrate). Such PsNs motion was brought about by a long-range force, i.e., thermal convection. Namely, thermal convection assists the supply of PsNs from outside of the irradiation area to inside of it. However, as shown by the trajectories in the figure, such PsNs were pushed away from the irradiation area. This behavior could be attributed to thermophoresis. By controlling thermophoresis and thermal convection, we succeeded in the formation of hexagonally close-packed PsNs.

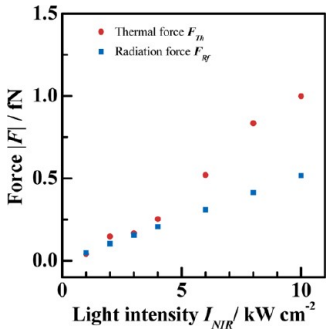

Figure 4. Numerical calculation of radiation force (blue squares) and thermal force (red circles) exerted on d = 0.1 μm PsNs at 10 nm far from the AR-NSL surface in a water solution.

2D Closely Packed Assembly Formation and Manipulation. As discussed above, we revealed that three kinds of physical force (radiation force, thermophoresis, and thermal convection) are involved in LSP excitation. By suppressing the repulsive force (thermophoresis), we can form a hexagonal assembly when PsNs are 2D closely packed on an AR-NSL substrate. Figure 6 shows representative optical micrographs of LSP-OT for 0.5 μm PsNs at I_{NIR} ∼ 2.0 kW/cm^2 (see also a movie available in the Supporting Information). Upon starting NIR irradiation, thermal convection assisted the collection of PsNs into the irradiation area. After that, PsNs were trapped on the substrate due to RF. During the trapping process, the PsNs spontaneously assembled with each other on the substrate. The size of the 2D assembly gradually increased with NIR irradiation time. Finally, a 2D closely packed hexagonal assembly was formed whose outline was almost consistent with the LSP excitation area. Stopping NIR irradiation immediately released the PsNs from the trapping area.

Utilizing such a stable trapping mechanism, we demonstrated smooth 2D manipulation of PsNs on the substrate. Figure 7 shows optical micrographs of manipulation trials where the PsNs assembly was rotated (see also the movie in the Supporting Information). NIR irradiation with a rectangular beam profile resulted in a rectangular assembly of 0.5 μm PsNs. Upon slowly rotating the rectangular-shaped focal spot (∼0.1 rad/s), the PsNs assembly was also moved along with the

dx.doi.org/10.1021/jp306405j | J. Phys. Chem. C 2013, 117, 2500−2506

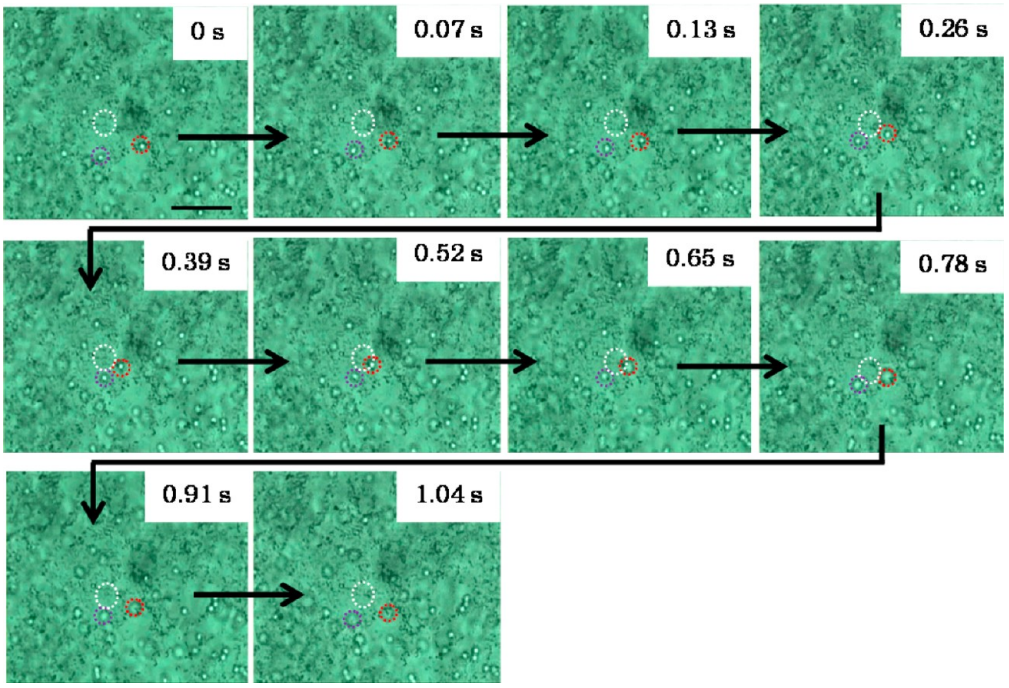

Figure 5. Optical micrographs of d = 1.0 μm PsNs dispersed in solution during NIR laser irradiation (20 kW/cm^2). The NIR laser was illuminated in the white dotted circle. The motion of the PsNs in the red and purple circles was tracked in each frame.

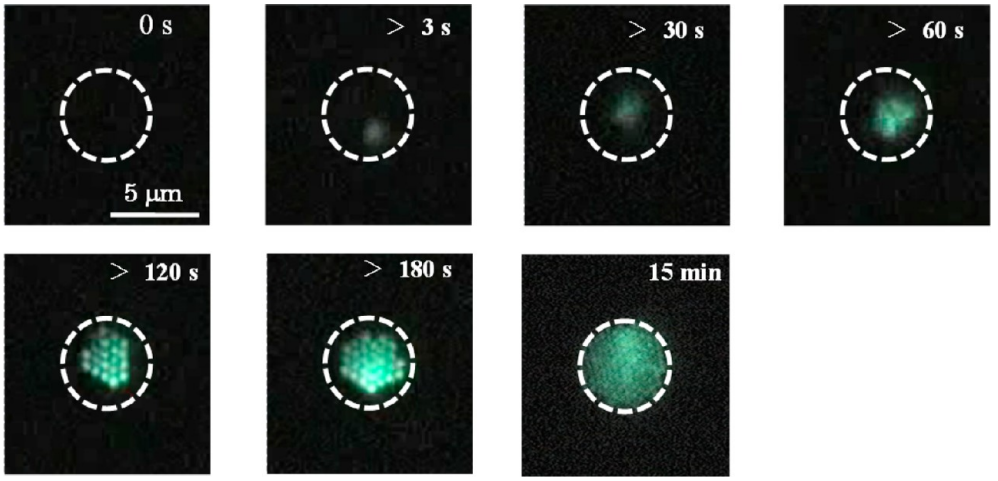

Figure 6. Optical micrographs of a closely packed assembly of d = 0.5 μm PsNs. The white circles noted by the dotted lines correspond to the LSP excitation area. The time duration of LSP excitation is given in each micrograph.

rotation of the NIR irradiation area. The formation of the rectangular assembly was also reversible by turning on and off the NIR irradiation. In comparison with recent studies on LSP-OT,[21,40,41] our method that is demonstrated here has three primary advantages: (i) PsNs were trapped and closely assembled within the LSP excitation area, (ii) a closely packed assembly of PsNs was formed with a desired shape by only changing the NIR beam profile, and (iii) the assembly could be freely manipulated on the plasmonic substrate. Such advantages were achieved with a simple optical setup and weak NIR light intensity. The LSP-OT could be a promising method for creating and manipulating 2D colloid crystals on a plasmonic substrate.

It should be noted that our technique is potentially extended for other nano/microparticles such as small metallic and semiconductor crystals. As Kotov et al. have demonstrated, self-organized nano/microassemblies of such particles can create advanced architectures with electronic/optical device function.[42,43] Our technique would be further applicable to assist the formation of such functional assemblies.

CONCLUSION

In conclusion, we investigated the optical trapping behavior of polystyrene nanospheres with gap-mode LSP-enhanced RF by means of confocal fluorescence microspectroscopy. We found that there is an optimum LSP excitation intensity for the stable trapping of the nanospheres. Above the optimum intensity, photothermal behavior such as thermophoresis disturbed the trapping process. These results were further supported by a numerical calculation of the radiation and thermal forces. Upon LSP excitation, thermal convection, which is also induced together with thermophoresis, supports LSP-OT through

dx.doi.org/10.1021/jp306405j | J. Phys. Chem. C 2013, 117, 2500−2506

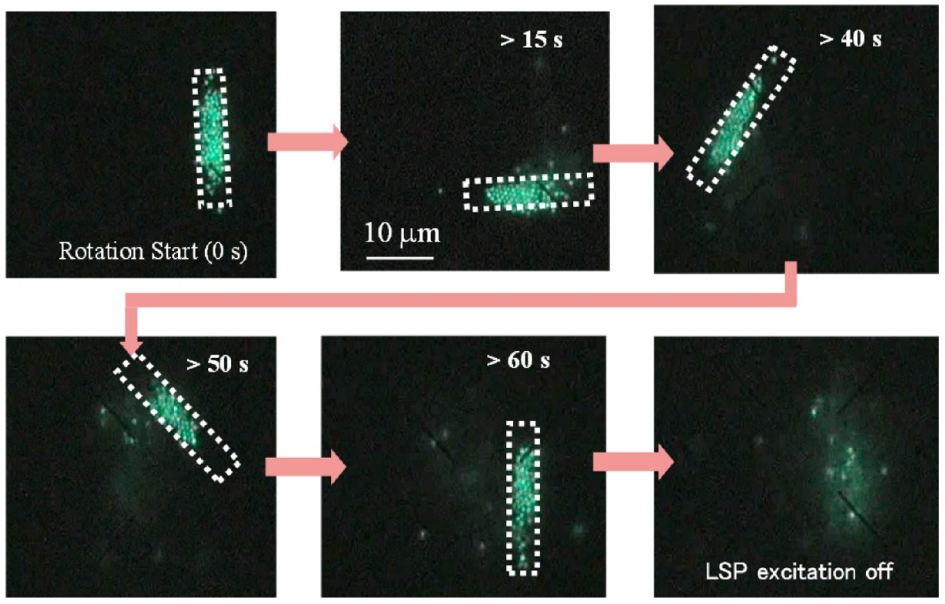

Figure 7. Optical micrographs of micropatterning and manipulation of d = 0.5 μm PsNs by scanning the NIR laser beam for LSP excitation. The rectangles noted by the dotted lines correspond to the LSP excitation area. The time duration of LSP excitation is given in each micrograph.

transportation of the nanospheres. Thus, control of three kinds of physical forces allows us to achieve optical trapping of nanospheres on a plasmonic substrate. Indeed, we demonstrated the 2D closely packed assembly of nanospheres. Furthermore, the smooth 2D manipulation of nanospheres was achieved. The method offers new opportunities to create and manipulate a 2D colloid crystal on a plasmonic substrate

■ ASSOCIATED CONTENT

Supporting Information

The configuration of AR-NSL substrate, the calculation method, and movies of LSP-OT. This material is available free of charge via the Internet at http://pubs.acs.org.

■ AUTHOR INFORMATION

Corresponding Author

*E-mail: twoboys@sci.hokudai.ac.jp.

Notes

The authors declare no competing financial interest.

■ ACKNOWLEDGMENTS

This work was partly supported by a Grant-in-Aid for Scientific Research from the Ministry of Education, Culture, Sports, Science and Technology of Japan for the Priority Area "Strong Photons-Molecules Coupling Fields (470)" (No. 19049004), No. 20550002, and the Global COE Program (Project No. B01: Catalysis as the Basis for Innovation in Materials Science). Y.T. and T.S. are very grateful to Laser System Ltd. for a financial support.

■ REFERENCES

(1) Takase, M.; Sawai, Y.; Nabika, H.; Murakoshi, K. *J. Photochem. Photobiol., A* **2011**, *221*, 169−174.
(2) Nagasawa, F.; Takase, M.; Nabika, H.; Murakoshi, K. *Chem. Commun.* **2011**, *47*, 4514−4516.
(3) Itoh, T.; Iga, M.; Tamaru, H.; Yoshida, K.; Biju, V.; Ishikawa, M. *J. Chem. Phys.* **2012**, *136*, 024703.
(4) Eustis, S.; El-Sayed, M. A. *Chem. Soc. Rev.* **2006**, *35*, 209−217.
(5) Kinkhabwala, A.; Yu, Z.; Fan, S.; Avlasevich, Y.; Müllen, K.; Moerner, W. E. *Nat. Photonics* **2009**, *3*, 654−657.
(6) Tsuboi, Y.; Shimizu, R.; Shoji, T.; Kitamura, N. *J. Am. Chem. Soc.* **2009**, *131*, 12623−12627.
(7) Ueno, K.; Takabatake, S.; Onishi, K.; Itoh, H.; Nishijima, Y.; Misawa, H. *Appl. Phys. Lett.* **2011**, *99*, 011107.
(8) Nishi, H.; Asahi, T.; Kobatake, S. *J. Phys. Chem. C* **2011**, *115*, 4564−4570.
(9) Geldhauser, T.; Ikegaya, S.; Kolloch, A.; Murazawa, N.; Ueno, K.; Boneberg, J.; Leiderer, P.; Scheer, E.; Misawa, H. *Plasmonics* **2011**, *6*, 207−212.
(10) El-Sayed, M. A. *J. Photochem. Photobiol., A* **2011**, *221*, 138−142.
(11) Halas, N. J. *Nano Lett.* **2010**, *10*, 3816−3822.
(12) Nabika, H.; Takase, M.; Nagasawa, F.; Murakoshi, K. *J. Phys. Chem. Lett.* **2010**, *1*, 2470−2487.
(13) Hashimoto, S.; Werner, D.; Uwada, T. *J. Photochem. Photobiol., C* **2012**, *13*, 28−54.
(14) Grigorenko, A. N.; Roberts, N. W.; Dickinson, M. R.; Zhang, Y. *Nat. Photonics* **2008**, *2*, 365−370.
(15) Righini, M.; Ghenuche, P.; Cherukulappurath, S.; Myroshnychenko, V.; García De Abajo, F. J.; Quidant, R. *Nano Lett.* **2009**, *9*, 3387−3391.
(16) Zhang, W.; Huang, L.; Santschi, C.; Martin, O. J. F. *Nano Lett.* **2010**, *10*, 1006−1011.
(17) Wang, K.; Schonbrun, E.; Steinvurzel, P.; Crozier, K. B. *Nat. Commun.* **2011**, *2*, 469.
(18) Çetin, A. E.; Yanik, A. A.; Yilmaz, C.; Somu, S.; Busnaina, A.; Altug, H. *Appl. Phys. Lett.* **2011**, *98*, 111110.
(19) Tanaka, Y.; Sasaki, K. *Appl. Phys. Lett.* **2012**, *100*, 021102.
(20) Chen, C.; Juan, M. L.; Li, Y.; Maes, G.; Borghs, G.; Van Dorpe, P.; Quidant, R. *Nano Lett.* **2012**, *12*, 125−132.
(21) Roxworthy, B. J.; Ko, K. D.; Kumar, A.; Fung, K. H.; Chow, E. K. C.; Liu, G. L.; Fang, N.; Toussaint, K. C. *Nano Lett.* **2012**, *12*, 796−801.
(22) Tsuboi, Y.; Shoji, T.; Kitamura, N.; Takase, M.; Murakoshi, K.; Mizumoto, Y.; Ishihara, H. *J. Phys. Chem. Lett.* **2010**, *1*, 2327−2333.
(23) Shoji, T.; Mizumoto, Y.; Ishihara, H.; Kitamura, N. *Jpn. J. Appl. Phys.* **2012**, *51*, 092001.
(24) Toshimitsu, M.; Matsumura, Y.; Shoji, T.; Kitamura, N.; Takase, M.; Murakoshi, K.; Yamauchi, H.; Ito, S.; Miyasaka, H.; Nobuhiro, A.; Mizumoto, Y.; Ishihara, H.; Tsuboi, Y. *J. Phys. Chem. C* **2012**, *116*, 14610−14618.

(25) Masuhara, H.; Sugiyama, T.; Rungsimanon, T.; Yuyama, K.; Miura, A.; Tu, J. *Pure Appl. Chem.* **2011**, *83*, 869−883.
(26) Tsuboi, Y.; Shoji, T.; Kitamura, N. *J. Phys. Chem. C* **2010**, *114*, 5589−5593.
(27) Messina, E.; Cavallaro, E.; Cacciola, A.; Iatì, M. A.; Gucciardi, P. G.; Borghese, F.; Denti, P.; Saija, R.; Compagnini, G.; Meneghetti, M.; Amendola, V.; Maragò, O. M. *ACS Nano* **2011**, *5*, 905−913.
(28) Junio, J.; Ng, J.; Cohen, J. A.; Lin, Z.; Ou-Yang, H. D. *Opt. Lett.* **2011**, *36*, 1497−1499.
(29) Usman, A.; Chiang, W.-Y.; Masuhara, H. *J. Photochem. Photobiol., A* **2012**, *234*, 83−90.
(30) Wu, J.; Gan, X. *Opt. Exp.* **2010**, *18*, 27619−27626.
(31) Qin, Z.; Bischof, J. C. *Chem. Soc. Rev.* **2012**, *41*, 1191−1217.
(32) Baffou, G.; Girard, C.; Quidant, R. *Phys. Rev. Lett.* **2010**, *104*, 136805.
(33) Biesso, A.; Qian, W.; El-Sayed, M. A. *J. Am. Chem. Soc.* **2008**, *130*, 3258−3259.
(34) Yokota, Y.; Ueno, K.; Misawa, H. *Small* **2011**, *7*, 252−258.
(35) Piazza, R.; Parola, A. *J. Phys.: Condens. Matter* **2008**, *20*, 153102.
(36) Piazza, R. *Soft Matter* **2008**, *4*, 1740−1744.
(37) Srinivasan, S.; Saghir, M. Z. *Int. J. Therm. Sci.* **2011**, *50*, 1125−1137.
(38) Braibanti, M.; Vigolo, D.; Piazza, R. *Phys. Rev. Lett.* **2008**, *100*, 108303.
(39) Kang, T.; Hong, S.; Choi, Y.; Lee, L. P. *Small* **2010**, *6*, 2649−2652.
(40) Roxworthy, B. J.; Toussaint, K. C. *Opt. Exp.* **2012**, *20*, 9591.
(41) Cuche, A.; Mahboub, O.; Devaux, E.; Genet, C.; Ebbesen, T. W. *Phys. Rev. Lett.* **2012**, *108*, 026801.
(42) Yang, M.; Sun, K.; Kotov, N. A. *J. Am. Chem. Soc.* **2010**, *132*, 1860−1872.
(43) Srivastava, S.; Santos, A.; Critchley, K.; Kim, K.-S.; Podsiadlo, P.; Sun, K.; Lee, J.; Xu, C.; Lilly, G. D.; Glotzer, S. C.; Kotov, N. A. *Science* **2010**, *327*, 1355−1359.